TRIM22 negatively regulates MHC-II expression

Ayano Inoue[1, 2], Masashi Watanabe[1], Takeshi Kondo[1], Satoshi Hirano[2] and Shigetsugu Hatakeyama[1,*]

[1]Department of Biochemistry, Faculty of Medicine and Graduate School of Medicine, Hokkaido University, Kita 15, Nishi 7, Kita-ku, Sapporo, Hokkaido 060-8638, Japan.

[2]Department of Gastroenterological Surgery II, Faculty of Medicine and Graduate School of Medicine, Hokkaido University, Kita 15, Nishi 7, Kita-ku, Sapporo, Hokkaido 060-8638, Japan.

***Correspondence:** Shigetsugu Hatakeyama, Department of Biochemistry, Faculty of Medicine and Graduate School of Medicine, Hokkaido University, Kita 15, Nishi 7, Kita-ku, Sapporo, Hokkaido 060-8638, Japan. Tel.:+81 11 706 5899; fax: +81 11 706 5169.

E-mail address: hatas@med.hokudai.ac.jp (S.Hatakeyama)

Highlights

- TRIM22 gene is strongly induced by IFN-γ stimulation.
- Gene knockout of TRIM22 leads to an increase of MHC-II proteins in U87MG cells.
- TRIM22 overexpression remarkably decreases MHC-II proteins in U87MG cell.
- TRIM22 may decrease MHC-II protein levels through a combination of multiple mechanisms other than transcription or degradation.

Abstract

The development of cancer treatment has recently achieved a remarkable breakthrough, and checkpoint blockade immunotherapy has received much attention. To enhance the therapeutic efficacy of checkpoint blockade immunotherapy, recent studies have revealed the importance of activation of $CD4^+$ T cells via an increase in major histocompatibility complex (MHC) class II molecules in cancer cells. Here, we demonstrate that tripartite motif-containing (TRIM) 22, negatively regulates MHC-II expression. Gene knockout of TRIM22 using Cas9-sgRNAs led to an increase of MHC-II proteins, while TRIM22 overexpression remarkably decreased MHC-II proteins. mRNA levels of MHC-II and class II transactivator (CIITA), which plays an essential role in the regulation of MHC-II transcription, were not affected by TRIM22. Furthermore, TRIM22 knockout did not suppress the degradation of MHC-II protein but rather promoted it. These results suggest that TRIM22 decreases MHC-II protein levels through a combination of multiple mechanisms other than transcription or degradation. We showed that inhibition of TRIM22 can increase the amount of MHC-II expression in cancer cells, suggesting a possibility of providing the biological basis for a possible therapeutic target to potentiate checkpoint blockade immunotherapy.

Abbreviations

CIITA, class II transactivator; PD-1, programed cell death-1; CTLA-4, cytotoxic T lymphocyte-associated molecule-4; MHC-I, MHC class I; MHC-II, MHC class II; APC,

antigen-presenting cell; HAT, histone acetyltransferase; IFN-γ, interferon-γ; STAT1, signal transducers and activators of transcription 1; PRR, pattern recognition receptor; MEM, Minimum Essential Medium; FBS, fetal bovine serum; HEK293T, human embryonic kidney 293T; ECL, enhanced chemiluminescence; PBS, phosphate-buffered saline; BSA, bovine serum albumin; CHX, Cycloheximide; MARCH1, Membrane-associated RING-CH-1; staf50, stimulated transacting factor 50 kDa; eIF4E, eukaryotic translation initiation factor 4E; TIL, tumor-infiltrating lymphocyte.

Keywords

TRIM22, MHC-II, ubiquitin, Checkpoint blockade immunotherapy, IFN-γ

1. Introduction

Cancer immunotherapies via attenuation of co-inhibitory receptors such as programed death-1 (PD-1) and cytotoxic T lymphocyte-associated molecule-4 (CTLA-4) have been developed in recent years [1]. These treatments, called checkpoint blockade immunotherapies, have become in therapies for a variety of cancers [2]. To exert their effects, recognition of tumor-specific antigens on surface MHC molecules by T cells is required. While MHC class I (MHC-I) molecules are broadly expressed in many kinds of cells and present peptides from endogenous proteins to $CD8^+$ T cells, MHC class II (MHC-II) molecules are normally found only on professional antigen-presenting cells (APCs) and peptides processed from exogenous proteins that are engulfed by APCs are presented to $CD4^+$ T cells [3]. Although the success of checkpoint receptor blocking antibodies has been thought to be mainly due to the effector functions of $CD8^+$ T cells, recent studies have shown that activation of $CD4^+$ T cells also plays an essential role in those treatments [4, 5]. It has also been reported that there is a positive correlation between MHC-II expression levels in cancer cells and therapeutic efficacy of checkpoint blockade immunotherapy [6, 7]. Thus, upregulation of MHC-II expression in cancer cells has been attracting attention as a new strategy for cancer treatment [8]. The expression of MHC-II genes is tightly controlled at the transcriptional level by its master regulator, CIITA [3, 9, 10]. CIITA is a transcriptional coactivator and recruits chromatin-modifying factors such as histone acetyltransferases (HATs) to MHC-II promoters, allowing an increase in MHC-II mRNA transcription [11]. Moreover, it is well known that MHC-II

expression is induced by several kinds of cytokines including interferon-γ (IFN-γ) [9]. IFN-γ stimulation induces recruitment of signal transducers and activators of transcription 1 (STAT1) to the CIITA promoter and thereby activates CIITA transcription [12-15].

TRIM family proteins are highly conserved E3 ubiquitin ligases, and more than 80 TRIM proteins have been identified in humans and mice [16]. Many TRIM proteins serve as critical regulators of various cellular processes including innate immunity, response to viral infection and cancer development [17, 18]. Many studies have shown that TRIM proteins function as regulators of inflammatory signals mediated by IFNs or pattern recognition receptors (PRRs). On the other hand, the involvement of TRIM proteins in the antigen presentation pathway via MHC to evoke adaptive immunity remains to be elucidated.

In this study, we systematically screened TRIM family genes induced by IFN-γ stimulation and identified TRIM22 as a one of the most strongly induced TRIM proteins by IFN-γ. TRIM22 overexpression downregulated the expression of MHC-II at the protein level and TRIM22 knockout upregulated the expression of MHC-II in glioblastoma cells. Our data indicate that TRIM22 functions as a negative regulator of MHC-II expression, suggesting that TRIM22 is one of the potential targets for checkpoint blockade immunotherapy.

2. Materials and methods

2.1. Cell culture

Human glioblastoma cells (U87MG cells) were maintained under an atmosphere of 5% CO_2 at 37°C in Eagle's Minimum Essential Medium (MEM) (Sigma-Aldrich, St. Louis, MI) supplemented with 10% fetal bovine serum (FBS) (Gibco BRL, Paisley, UK), and human embryonic kidney 293T (HEK293T) cells were maintained in Dulbecco's modified Eagle's medium (DMEM) (Sigma-Aldrich) supplemented with 10% fetal bovine serum (FBS).

2.2. Establishment of stable transfectants by using a retrovirus expression system

Complementary DNAs encoding FLAG-tagged TRIM22 or FLAG-tagged TRIM21 and the corresponding empty plasmid were subcloned into pQCXI-puro (Takara, Shiga, Japan). The resulting vectors were used for transfection into HEK293T cells and then recombinant retroviruses were generated. Forty-eight h after transfection, culture supernatants were harvested and then used for infection. The infection was carried out in the presence of polybrene (8 μg/ml, Sigma) and the infected cells were expanded in a medium containing puromycin (1 μg/ml, Sigma).

2.3. Transfection and immunoblot analysis

TRIM22 knockout cells were generated with CRISPR/Cas9-based genome editing technology. Two target sequences of guide RNA were designed using GPP sgRNA Designer and inserted into the pSpCas9 (BB)-2A-Puro (PX459) V2.0 vector, a gift from Feng Zhang. U87MG cells were transiently transfected with these plasmids using Polyethylenimine Max (Polyscience, 24765) as a carrier. Twenty-four h after transfection, the cells were treated with 1 μg/ml puromycin (Invitrogen) for 48 h. Puromycin-resistant cells were collected and cloned in 96-well plates. KO screening was performed by immunoblot analysis. To confirm genome editing, the target site DNA sequence in the genome of candidate clones was amplified by PCR using KOD FX DNA polymerase (KFX-101, Toyobo) and was purified with ExoSAP-IT Express PCR Cleanup Reagents (75001, Thermo Fisher Scientific), followed by DNA sequencing (BigDye Terminator v1.1, 4337452, Thermo Fisher Scientific). The following primers were used for PCR and DNA sequencing: 5'-AACCTCTGAGCCTAGATTGTG-3' (forward primer) and 5'-AACCTCTGAGCCTAGATTGTG-3' (reverse primer).

Immunoblot analysis was performed with primary antibodies, horseradish peroxidase-conjugated antibodies to mouse or rabbit immunoglobulin G (Promega, Madison, WI, 1:15,000 dilution) and an enhanced chemiluminescence (ECL) reagent (Thermo Scientific). The following primary antibodies were used: anti-FLAG M2 (Sigma-Aldrich, 1:2,000 dilution), anti-HLA-DP/DR (HL-40, exbio, Praha, Czech Republic, 1:1,000 dilution), anti-HLA-DR (TAL1B5, Santa Cruz Biotechnology, Dallas, TX, 1:200 dilution), anti-HLA-DR (G-7, Santa Cruz Biotechnology, 1:200 dilution), anti-

TRIM22 (Atlas Antibodies, Sweden, 1:1,000 dilution), anti-CIITA (Cell Signaling Technology, Danvers, MA, 1:1,000 dilution), anti-mTOR (7C10, Cell Signaling Technology, 1:1,000 dilution), anti-Raptor (24C12, Cell Signaling Technology, 1:1,000 dilution), anti-Rictor (53A2, Cell Signaling Technology, 1:1,000 dilution), anti-GβL (86B8, Cell Signaling Technology, 1:1,000 dilution) and anti-GAPDH (Thermo Scientific, 1:100,000 dilution).

2.4. RNA extraction and real-time PCR

Total RNA was prepared using the Rneasy Mini kit (Qiagen, Hilden, Germany) in accordance with the manufacturer's protocol. RNA was eluted with 50 μl of Rnase-free distilled water. The concentration of RNA was determined by using a Nanodrop. RNA was reverse transcribed into cDNA using the ReverTra Ace qPCR RT Kit (Toyobo Life Science, Shanghai, China) according to the manufacturer's protocols. cDNA was subjected to real-time PCR in a 20-μl reaction mixture with Power SYBR Green PCR Master Mix (Thermo Fisher Scientific) on a real-time sequence detection system (ABI Step One Plus, Thermo Fisher Scientific). Each expression level was calculated following normalization to GAPDH levels by the comparative ΔΔ threshold cycle method. The specificity of the amplification reactions was confirmed by melt curve analysis. Results shown are representative of three independent experiments. The primers used for PCR are listed in Supplementary Table 1.

2.5. Flow cytometry

Immunofluorescent staining was performed in microtubes. Dilutions and washings were performed throughout in phosphate-buffered saline (PBS) containing 0.1% bovine serum albumin (BSA) and 0.1% NaN_3, referred to as FACS medium. Approximately 10^6 cells per sample were suspended in 100 μl of FACS medium with anti-HLA-DP/DR at a dilution of 1:100 and incubated on ice for 1 h. The cells were washed twice in 200 μl of FACS medium and then incubated again on ice for 30 min with an Alexa790-labeled goat polyclonal antibody to mouse immunoglobulin (Invitrogen) at a dilution of 1:200. The cells were rewashed twice and resuspended in 500 μl of FACS medium containing 7-aminoactinomycin D (Invitrogen). Flow cytometry analysis was performed on 20,000 events using a BD FACSCanto™II cytometer and data were analyzed using BD FACSDiva™ software (Becton-Dickinson, Mountain View, Canada).

2.6. Cycloheximide (CHX) chase assay

CHX (25 μg/ml, Sigma-Aldrich, St Louis, MO) was introduced to the culture medium to inhibit translation and cell lysates were prepared at the indicated times. The cell lysates were examined using immunoblot analysis. Densitometric analysis was carried out using NIH-ImageJ™.

2.7. Immunofluorescence staining

Cells grown on a glass cover were fixed with 4% paraformaldehyde in PBS and incubated at 37℃ with 5% CO_2 for 30 min and then incubated for 1 h at room temperature with a primary antibody to HLA-DR (0.125 μg/ml, LN3, Bethyl Laboratories, Montgomery, TX) in PBS containing 0.1% BSA. The cells were then incubated with an Alexa488-labeled goat polyclonal antibody to mouse immunoglobulin (Invitrogen) at a dilution of 1:1,000 for 1 h at room temperature. The cells were covered with a drop of ProLong Diamond Antifade Mountant with DAPI (Invitrogen) and then imaged on a Zeiss LSM 710 confocal microscope (Carl Zeiss Microscopy GmbH, Germany). For quantitation, 20 wild-type cells or TRIM22 knockout cells were imaged and the plasma membrane area of each cell was manually marked. The threshold level at which MHC-II antibody fluorescence intensity was higher than the background was determined and the total fluorescence intensity of each area was quantitated by LSM710.

2.8. Sample preparation for mass spectrometry analysis

HEK293T cells (5.0×10^7) that stably expressed FLAG-tagged TRIM22 were lysed in a solution containing 50 mM Tris-HCl (pH 7.6), 300 mM NaCl, 10% glycerol, 0.2% NP-40, 10 mM iodoacetamide (Sigma-Aldrich), 10 mM N-ethylmaleimide (Sigma-Aldrich), 0.5 mM 4-(2-aminoethyl)-benzenesulfonyl fluoride hydrochloride (AEBSF, Roche, Branchburg, NJ), 10 μM MG132 (Merck, Darmstadt, DE), and PhosStop phosphatase inhibitors (Sigma-Aldrich). The cell lysates were sonicated and centrifuged

at 20,000×g for 10 min at 4°C, and the resulting supernatant was incubated with anti-FLAG M2 agarose (Sigma-Aldrich) for 2 h at 4°C. The resin was separated by centrifugation, washed five times with ice-cold lysis buffer, and eluted twice with 50 μl of lysis buffer containing 0.25 mg/ml FLAG peptide (Sigma-Aldrich). Eluted peptides were dried by vacuum centrifugation, reduced (55 mM dithiothreitol, 5 min at 95°C) (Thermo Fisher Scientific), alkylated (10 mM iodoacetamide, 20 min at room temperature in the dark) (Thermo Fisher Scientific), and digested with trypsin (50 ng/μl, overnight at 37°C) (Promega) using 0.01% RapiGest SF (Waters). After tryptic digestion, the samples were acidified with TFA and desalted by solid-phase extraction using GL-Tip GC and GL-Tip SDB (GL Sciences, Tokyo, Japan).

2.9. Mass spectrometry analysis

Desalted tryptic digests were analyzed by nanoflow ultra-HPLC (EASY-nLC 1000; Thermo Fisher Scientific) on-line coupled to an Orbitrap Elite instrument (Thermo Fisher Scientific). The mobile phases were 0.1% formic acid in water (solvent A) and 0.1% formic acid in 100% acetonitrile (solvent B). Peptides were directly loaded onto a C18 Reprosil analytical column (3 μm in particle size, 75 μm in i.d., and 12 cm in length; Nikkyo Technos, Tokyo, Japan) and separated using a 150-min two-step gradient (0-35% for 130 min, 35-100% for 5 min, and 100% for 15 min of solvent B) at a constant flow rate of 300 nL/min. For ionization, a liquid junction voltage of 1.6 kV and a capillary temperature of 200°C were used. The Orbitrap Elite instrument was operated in the data-

dependent MS/MS mode using Xcalibur software (Thermo Fisher Scientific) with survey scans acquired at a resolution of 120,000 at m/z 400. The top 10 most abundant isotope patterns with a charge ranging from 2 to 4 were selected from the survey scans with an isolation window of 2.0 m/z and fragmented by collision-induced dissociation with normalized collision energies of 35. The maximum ion injection times for the survey and MS/MS scans were 60 ms, and the ion target values were set to 1e6 for the survey and MS/MS scans.

2.10. Protein identification from MS data

Proteome Discoverer software (version 2.4; Thermo Fisher Scientific) was used to generate peak lists. The MS/MS spectra were searched against a UniProt Knowledgebase (version 2017_10) using the SequestHT search engine. The precursor and fragment mass tolerances were set to 10 ppm and 0.6 Da, respectively. Methionine oxidation, protein amino-terminal acetylation, Asn/Gln deamidation, Ser/Thr/Tyr phosphorylation, diglycine modification of Lys side chains, and Cys carbamidomethyl modification were set as variable modifications for database searching. Peptide identification was filtered at a 1% false discovery rate. Label-free quantification (LFQ) was calculated using the intensities of precursor ions in the precursor ions quantifier node. Normalization was performed so that the sum of the abundance values for all peptides in each sample was the same. For statistical analyses of MS data, the *P* values in a volcano plot were determined by unpaired, two-sided Student's *t*-test. Proteins with an average PSMs of <3

in the FLAG-TRIM22 samples were filtered out.

2.11. Statistical analysis

Cell fluorescence quantification was analyzed by Dunnett's test after one-way analysis of variance (ANOVA). In each analysis, differences were statistically considered significant if the *p* value was less than 0.05.

3. Results

3.1. TRIM22 transcription is upregulated by IFN-γ

While the constitutive expression of MHC-II genes is restricted to a few cell types, including immune cells such as macrophages, dendritic cells, and B-cells and some tumor cells such as melanoma, colorectal cancer and glioma cells, IFN-γ treatment induces MHC-II expression in many cell types, not limited to the above cells [19]. We first searched for TRIM family members that were induced by IFN-γ stimulation. We examined mRNA levels of TRIM genes in HEK293T cells that were treated with IFN-γ and found that some TRIM genes including TRIM22, TRIM21, TRIM5α, TRIM74 and TRIM15 were significantly upregulated (Fig. 1A). We further examined the expression of these TRIM genes in U87MG human glioma cells, which constitutively express MHC-II. We found that the expression of TRIM22, TRIM21, and TRIM5α was upregulated and that the TRIM22 gene was most strongly induced in U87MG cells (Fig. 1B). Immunoblot analysis also verified the remarkable increase of TRIM22 protein in U87MG cells with IFN-γ stimulation (Fig. 1C). We therefore decided to focus on the relationship between TRIM22 and MHC-II expression.

3.2. TRIM22 overexpression suppresses the expression of MHC-II protein

We established U87MG cells that stably expressed FLAG-tagged TRIM22 with a

retroviral expression system (Fig. 2A). Immunoblot analysis showed that MHC-II proteins were remarkably decreased in TRIM22-introduced cells (Fig. 2B). We checked the surface expression of MHC-II on the cells by flow cytometry, and flow cytometric analysis also showed a decrease of MHC-II protein levels on the surface of TRIM22-overexpressed cells (Fig. 2C). These results indicated that ectopic expression of TRIM22 downregulated the expression of MHC-II proteins. On the other hand, although the induction of TRIM21 by IFN-γ was equally strong as that of TRIM22, MHC-II protein level was unchanged in TRIM21-overexpressed cells (Fig. 2D).

To verify whether TRIM22 affects the expression of MHC-II levels via the expression of other family members, we analyzed the mRNA expression levels of all TRIM members in U87MG cells stably expressing FLAG-TRIM22, and we found that TRIM58, TRIM54 and TRIM50 were upregulated in TRIM22-overexpressing cells (Supplementary Fig. 1). However, there has been no report of the involvement of these genes including TRIM58, TRIM54 and TRIM50 in the regulation of MHC class II expression.

3.3. TRIM22 knockout promotes the expression of MHC-II protein

We next established TRIM22-knockout U87MG cells with CRISPR/Cas9-based genome editing technology (Fig. 3A). Immunoblot analysis showed that MHC-II protein was increased in TRIM22-knockout cells compared with that in wild-type cells with or without IFN-γ stimulation, but CIITA, which plays an essential role in the regulation of

MHC class II gene transcription, was not changed (Fig. 3B). Since the antibody (clone HL-40) recognizes both HLA-DP and HLA-DR, we also used two different monoclonal antibodies that specifically recognize HLA-DR. HLA-DR protein was increased more in TRIM22-knockout cells than in wild-type cells under an unstimulated condition, whereas there was no difference in the rates of increase in HLA-DR expression levels among these cells under the condition of IFN-γ stimulation, suggesting that HLA-DP increased more with IFN-γ stimulation in TRIM22-knockout cells (Fig. 3B). MHC-II expression in wild-type U87MG cells and TRIM22-knockout U87MG cells was also examined using flow cytometry (Fig. 3C). Compared with the wild-type cells, the expression of MHC-II on the cell surface was increased in TRIM22-knockout cells. U87MG cells are one of the cell lines that upregulate MHC-II expression in response to IFN-γ. Although MHC-II expression on the cell surface of both wild-type and TRIM22-knockout cells was increased by IFN-γ treatment, the expression level was significantly higher in TRIM22-knockout cells than in wild-type cells (Fig. 3C). We next performed immunofluorescence staining of MHC-II expression on TRIM22-knockout cells. Consistent with the results of flow cytometry analysis, the amount of MHC-II on the cell surface was remarkably increased in TRIM22-knockout cells compared with that in wild-type cells, especially in the presence of IFN-γ stimuli (Fig. 3D and E).

3.4. TRIM22 neither affects the transcription of MHC-II mRNAs nor suppresses degradation of MHC-II proteins

We investigated the mRNA levels of MHC-II and CIITA, the master regulator of MHC-II, in wild-type and TRIM22-knockout cells by qRT-PCR. While mRNAs in both cell lines were induced by IFN-γ stimulation, there was no significant difference between wild-type cells and TRIM22-knockout cells (Fig. 4).

To further explore the mechanism by which MHC-II expression is regulated by TRIM22, we examined the protein stability of MHC-II. It is known that the stability of MHC-II protein is regulated by E3 ubiquitin ligases. Membrane-associated RING-CH-1 (MARCH1), one of well-known regulators, ubiquitinates MHC-II and then leads to lysosomes for degradation [20-22]. We hypothesized that TRIM22 regulates MHC-II via degradation in the same manner as MARCH1 and we performed a protein degradation assay using cycloheximide as a translation inhibitor. We treated wild-type and TRIM22-knockout cells with cycloheximide for the indicated times. The results showed that TRIM22 knockout did not suppress the degradation of MHC-II protein but rather promoted it (Fig. 5A and B). These results suggested that TRIM22 decreases MHC-II protein level through a mechanism other than degradation. Furthermore, to elucidate the molecular mechanism by which MHC-II protein expression is suppressed by TRIM22, we immunoprecipitated and identified FLAG-TRIM22-interacting proteins from cell lysates by LC-MS/MS analysis (Supplementary Fig. 2A). mTOR, which is a key regulator of mRNA translation, was included as one of the TRIM22-binding protein candidates, and immunoprecipitation experiments revealed that TRIM22 interacted with mTOR and other mTOR subunits in HEK293T cells (Supplementary Fig. 2B) and in U87MG cells (Supplementary Fig. 2C), suggesting that TRIM22 regulates MHC-II mRNA translation

via the mTOR/4E-BP1/eIF4E axis.

4. Discussion

IFN-γ treatment induces MHC-II expression via CIITA in many cell types. In this study, we showed that TRIM22 suppresses MHC-II expression. We also demonstrated that many TRIM family members were induced by IFN-γ stimulation and that TRIM22 was one of the most strongly induced TRIM family genes. These results suggest that one of the physiological roles of TRIM22 in this pathway is to suppress the amount of MHC-II protein in a negative feedback manner and to limit the extent of MHC-II induction.

TRIM22, also called staf50 (stimulated transacting factor 50 kDa), is a member of the TRIM family of proteins that are involved in anti-viral activity. TRIM22 was first identified as a restriction factor against HIV-1 transcription, and several studies have shown that TRIM22 affects the infection of some other viruses including influenza A virus, hepatitis B and C viruses, rubella virus, Epstein-Barr virus, human papillomavirus and encephalo-myocarditis virus [23-26]. Although many studies have shown a crucial aspect of TRIM22 for resistance to pathogens, the involvement of TRIM22 in the regulation of MHC expression has not been demonstrated. We found that knockout of TRIM22 increased the protein level of MHC-II. However, TRIM22 did not affect the mRNA levels of MHC-II and CIITA, suggesting that TRIM22 does not regulate the expression of MHC-II at the transcriptional level. We also showed that the stability of MHC-II protein was decreased in TRIM22-knockout cells, although this result seemed to compete with the fact that TRIM22 negatively regulated MHC-II protein levels. Thus, there should be a mechanism other than transcription or degradation to explain the

decrease of MHC-II protein. In the process of translation, the eukaryotic translation initiation factor 4E (eIF4E), which regulates the process of initiation, interacts with the scaffolding protein eIF4G, which binds to the helicase eIF4A, to form the eIF4F complex, allowing to the initiation of the cap-dependent translation [27]. It has been reported that TRIM22 inhibits the binding of eIF4E to eIF4G and represses cap-dependent translation [28]. Moreover, we found that TRIM22 interacts with the mTOR complex, which regulates mRNA translation via phosphorylation of 4E-BP1 and p70 S6 kinase. Therefore, there is a possibility that TRIM22-mediated MHC-II expression is regulated through the eIF4E/eIF4G or mTOR/4E-BP1/eIF4E axis (Fig. 5C).

The transport of MHC-II to the cell surface is another point to be discussed. Both the intracellular total protein amount and the cell surface protein amount of MHC-II were increased in TRIM22-knockout cells with or without IFN-γ stimulation. However, the increment in the amount of surface MHC-II was not greatly different or smaller than the increment in the amount of total MHC-II under the condition of IFN-γ stimulation, while the increment in the amount of surface MHC-II in TRIM22-knockout cells was larger than the increment in the amount of total MHC-II in TRIM22-knockout cells without IFN-γ stimulation. Actually, the results obtained by immunofluorescent staining showed that a large amount of MHC-II molecules in wild-type cells remained in the intracellular vesicle-like structure without IFN-γ stimulation, whereas MHC-II was mainly observed on the cell surface in TRIM22-knockout cells (Fig. 3D, upper panel). Most of the MHC-II protein was observed on the cell surface both in wild-type cells and TRIM22-knockout cells with IFN-γ stimulation (Fig. 3D, lower panel). Therefore, TRIM22 may also

suppress the transport of MHC-II to the cell surface without IFN-γ.

Some studies have revealed that MHC-II expression in tumor cells was associated with a better outcome in patients who received anti-PD-1 therapy for certain cancers. For example, melanomas with constitutive tumor cell-autonomous MHC-II/HLA-DR expression are associated with a high level of infiltration of $CD4^+$ and $CD8^+$ T cells in cancer lesions and enhanced response to PD-1-targeted immunotherapy [7, 19]. Clinical remissions have been observed in melanoma patients treated with $CD4^+$ T cells expanded *ex vivo* in the presence of tumor antigens [6]. MHC-II-positive breast tumors were found to have a greater degree of tumor-infiltrating lymphocytes (TILs) after neoadjuvant chemotherapy, and the greater degree of TILs correlated with improved outcomes after surgical resection, suggesting that MHC-II expression is an important biomarker in breast cancer [29]. Moreover, in a MHC-II-negative ovarian cancer model, enforced expression of MHC-II has been shown to result in increased antitumor inflammation, Th1 differentiation and induction of antigen-specific $CD4^+$ T cells [6]. Although PD-1 immunotherapy provides durable disease control in many patients, both intrinsic resistance and adaptive resistance are emerging [30]. A combination of PD-1 and LAG-3 or FCRL6 blockades may augment the therapeutic response for MHC-II-expressing tumors [29].

Based on our results showing that TRIM22 suppresses MHC-II expression, there is a possibility that TRIM22 is involved in the mechanism of the intrinsic low MHC-II expression level in certain cancers. Infiltrating Th1 cells within the tumor microenvironment often produce proinflammatory cytokines such as IFN-γ. IFN-γ

generally promotes MHC-II expression in many cells, but some cancer cells do not respond to IFN-γ. TRIM22 may also be involved in this situation. Increasing the expression of MHC-II is an important strategy for cancer therapy including checkpoint blockade immunotherapy. Our findings may provide TRIM22 as a novel therapeutic target for efficient checkpoint blockade immunotherapy.

Availability of data and materials

The mass spectrometric datasets are available in ProteomeXchange under the accession number PXD033731 via the jPOST repository. The data and materials used in this research are available from the corresponding author upon reasonable request.

CRediT authorship contribution statement

Ayano Inoue: Conceptualization, Data Curation, Formal analysis, Investigation, Writing–Original Draft.

Masashi Watanabe: Conceptualization, Data Curation, Formal analysis, Funding acquisition, Investigation, Supervision, Writing–Review & Editing.

Takeshi Kondo: Data Curation, Formal analysis.

Satoshi Hirano: Supervision, Writing–Review & Editing.

Shigetsugu Hatakeyama: Conceptualization, Project administration, Supervision, Writing–Review & Editing

Funding

This work was supported in part by KAKENHI from the Ministry of Education, Culture, Sports, Science and Technology in Japan (to 17H05784, 19H05280, 21H00266 and 21H02674 to SH; 17H05989, 19K22408, and 21H02690 to MW) and by the YASUDA Medical Foundation (MW), Suzuken Memorial Foundation (MW), the Japan Heart Foundation Dr. Hiroshi Irisawa & Dr. Aya Irisawa Memorial Research Grant (MW), Futaba Electronics Memorial Foundation (MW), the Nagao Memorial Fund (MW), the

Suhara Foundation (MW), Takeda Science Foundation (MW), SEI Group CSR Foundation (MW), Foundation for Promotion of Cancer Research in Japan (MW), and Kobayashi Foundation for Cancer Research (MW).

Declaration of interest

The authors declare that they have no known competing financial interests or personal relationships that could have appeared to influence the work reported in this paper.

Acknowledgments

We would like to thank Dr. Feng Zhang for providing plasmids and Mr. Takahiro Asanuma and Ms. Yumi Matsuzaki and Ms. Siho Sakata for help in preparing the manuscript.

References

[1] A. Ribas, J.D. Wolchok, Cancer immunotherapy using checkpoint blockade, Science, 359 (2018) 1350-1355.

[2] G.L. Beatty, W.L. Gladney, Immune escape mechanisms as a guide for cancer immunotherapy, Clin Cancer Res, 21 (2015) 687-692.

[3] P.J. van den Elsen, Expression regulation of major histocompatibility complex class I and class II encoding genes, Front Immunol, 2 (2011) 48.

[4] A.D. Waldman, J.M. Fritz, M.J. Lenardo, A guide to cancer immunotherapy: from T cell basic science to clinical practice, Nat Rev Immunol, 20 (2020) 651-668.

[5] M. de Charette, A. Marabelle, R. Houot, Turning tumour cells into antigen presenting cells: The next step to improve cancer immunotherapy?, Eur J Cancer, 68 (2016) 134-147.

[6] J. Thibodeau, M.C. Bourgeois-Daigneault, R. Lapointe, Targeting the MHC Class II antigen presentation pathway in cancer immunotherapy, Oncoimmunology, 1 (2012) 908-916.

[7] D.B. Johnson, M.V. Estrada, R. Salgado, V. Sanchez, D.B. Doxie, S.R. Opalenik, A.E. Vilgelm, E. Feld, A.S. Johnson, A.R. Greenplate, M.E. Sanders, C.M. Lovly, D.T. Frederick, M.C. Kelley, A. Richmond, J.M. Irish, Y. Shyr, R.J. Sullivan, I. Puzanov, J.A. Sosman, J.M. Balko, Melanoma-specific MHC-II expression represents a tumour-autonomous phenotype and predicts response to anti-PD-1/PD-L1 therapy, Nat Commun, 7 (2016) 10582.

[8] S.J. Rodig, D. Gusenleitner, D.G. Jackson, E. Gjini, A. Giobbie-Hurder, C. Jin, H. Chang, S.B. Lovitch, C. Horak, J.S. Weber, J.L. Weirather, J.D. Wolchok, M.A. Postow, A.C. Pavlick, J. Chesney, F.S. Hodi, MHC proteins confer differential sensitivity to CTLA-4 and PD-1 blockade in untreated metastatic melanoma, Sci Transl Med, 10 (2018).

[9] R. Romieu-Mourez, M. Francois, M.N. Boivin, J. Stagg, J. Galipeau, Regulation of MHC class II expression and antigen processing in murine and human mesenchymal stromal cells by IFN-gamma, TGF-beta, and cell density, J Immunol, 179 (2007) 1549-1558.

[10] N.M. Choi, P. Majumder, J.M. Boss, Regulation of major histocompatibility complex class II genes, Curr Opin Immunol, 23 (2011) 81-87.

[11] C. Spilianakis, J. Papamatheakis, A. Kretsovali, Acetylation by PCAF enhances CIITA nuclear accumulation and transactivation of major histocompatibility complex class II genes, Mol Cell Biol, 20 (2000) 8489-8498.

[12] A.C. Morris, G.W. Beresford, M.R. Mooney, J.M. Boss, Kinetics of a gamma interferon response: expression and assembly of CIITA promoter IV and inhibition by methylation, Mol Cell Biol, 22 (2002) 4781-4791.

[13] K.L. Wright, J.P. Ting, Epigenetic regulation of MHC-II and CIITA genes, Trends Immunol, 27 (2006) 405-412.

[14] W. Reith, S. LeibundGut-Landmann, J.M. Waldburger, Regulation of MHC class II gene expression by the class II transactivator, Nat Rev Immunol, 5 (2005) 793-806.

[15] A. Muhlethaler-Mottet, L.A. Otten, V. Steimle, B. Mach, Expression of MHC class

II molecules in different cellular and functional compartments is controlled by differential usage of multiple promoters of the transactivator CIITA, EMBO J, 16 (1997) 2851-2860.

[16] K. Ozato, D.M. Shin, T.H. Chang, H.C. Morse, 3rd, TRIM family proteins and their emerging roles in innate immunity, Nat Rev Immunol, 8 (2008) 849-860.

[17] S. Hatakeyama, TRIM Family Proteins: Roles in Autophagy, Immunity, and Carcinogenesis, Trends Biochem Sci, 42 (2017) 297-311.

[18] S. Hatakeyama, TRIM proteins and cancer, Nat Rev Cancer, 11 (2011) 792-804.

[19] M.L. Axelrod, R.S. Cook, D.B. Johnson, J.M. Balko, Biological Consequences of MHC-II Expression by Tumor Cells in Cancer, Clin Cancer Res, 25 (2019) 2392-2402.

[20] A. De Gassart, V. Camosseto, J. Thibodeau, M. Ceppi, N. Catalan, P. Pierre, E. Gatti, MHC class II stabilization at the surface of human dendritic cells is the result of maturation-dependent MARCH I down-regulation, Proc Natl Acad Sci U S A, 105 (2008) 3491-3496.

[21] K.R. Wilson, H. Liu, G. Healey, V. Vuong, S. Ishido, M.J. Herold, J.A. Villadangos, J.D. Mintern, MARCH1-mediated ubiquitination of MHC II impacts the MHC I antigen presentation pathway, PLoS One, 13 (2018) e0200540.

[22] Y. Matsuki, M. Ohmura-Hoshino, E. Goto, M. Aoki, M. Mito-Yoshida, M. Uematsu, T. Hasegawa, H. Koseki, O. Ohara, M. Nakayama, K. Toyooka, K. Matsuoka, H. Hotta, A. Yamamoto, S. Ishido, Novel regulation of MHC class II function in B cells, EMBO J, 26 (2007) 846-854.

[23] C.J. Hattlmann, J.N. Kelly, S.D. Barr, TRIM22: A Diverse and Dynamic Antiviral Protein, Mol Biol Int, 2012 (2012) 153415.

[24] Q. Lian, B. Sun, Interferons command Trim22 to fight against viruses, Cell Mol Immunol, 14 (2017) 794-796.

[25] S.D. Barr, J.R. Smiley, F.D. Bushman, The interferon response inhibits HIV particle production by induction of TRIM22, PLoS Pathog, 4 (2008) e1000007.

[26] E. Vicenzi, G. Poli, The interferon-stimulated gene TRIM22: A double-edged sword in HIV-1 infection, Cytokine Growth Factor Rev, 40 (2018) 40-47.

[27] I.S. Amorim, G. Lach, C.G. Gkogkas, The Role of the Eukaryotic Translation Initiation Factor 4E (eIF4E) in Neuropsychiatric Disorders, Front Genet, 9 (2018) 561.

[28] J. Petersson, M. Ageberg, C. Sanden, T. Olofsson, U. Gullberg, K. Drott, The p53 target gene TRIM22 directly or indirectly interacts with the translation initiation factor eIF4E and inhibits the binding of eIF4E to eIF4G, Biol Cell, 104 (2012) 462-475.

[29] D.B. Johnson, M.J. Nixon, Y. Wang, D.Y. Wang, E. Castellanos, M.V. Estrada, P.I. Ericsson-Gonzalez, C.H. Cote, R. Salgado, V. Sanchez, P.T. Dean, S.R. Opalenik, D.M. Schreeder, D.L. Rimm, J.Y. Kim, J. Bordeaux, S. Loi, L. Horn, M.E. Sanders, P.B. Ferrell, Jr., Y. Xu, J.A. Sosman, R.S. Davis, J.M. Balko, Tumor-specific MHC-II expression drives a unique pattern of resistance to immunotherapy via LAG-3/FCRL6 engagement, JCI Insight, 3 (2018).

[30] A. Pedoeem, I. Azoulay-Alfaguter, M. Strazza, G.J. Silverman, A. Mor, Programmed

death-1 pathway in cancer and autoimmunity, Clin Immunol, 153 (2014) 145-152.

Figure legends

Fig. 1. TRIM22 expression induced by IFN-γ. (A) The mRNA expression of all TRIM genes was analyzed by qRT-PCR. The relative gene log2 expression changes are presented as a heat map. Expression levels in HEK293T cells treated with IFN-γ (1,000 units/ml) for 24 h relative to Mock treatment were normalized for each TRIM gene. Green and red colors indicate lower levels and higher levels of gene expression, respectively. (B) qRT-PCR analysis of TRIM mRNA levels in U87MG cells treated with IFN-γ (1,000 units/ml) for 24 h. The top five TRIM genes in Fig. 1A were analyzed. Expression level of each gene was normalized to that of GAPDH. Shown are the means ± SDs from three independent experiments. (C) Immunoblot analysis of TRIM22 protein in U87MG cells treated with IFN-γ (1,000 units/ml) for 24 h. Anti-GAPDH antibody was used as an internal control.

Fig. 2. Overexpression of TRIM22 inhibits MHC-II expression. (A) Establishment of U87MG cell lines stably expressing FLAG-tagged TRIM22. U87MG cells were infected with a retrovirus encoding FLAG-tagged TRIM22 and the corresponding control vector (Mock). Each expression level of TRIM22 protein was verified by immunoblot analysis. Anti-GAPDH antibody was used as an internal control. (B) Immunoblot analysis of MHC-II protein in U87MG cell lines expressing FLAG-tagged TRIM22 and the corresponding control. Anti-GAPDH antibody was used as an internal control. (C) Flow cytometric analysis of cell surface MHC-II expression in U87MG cell lines expressing

FLAG-tagged TRIM22 and the corresponding control. Gray: Mock, Blue: FLAG-TRIM22. (D) Immunoblot analysis of MHC-II protein in U87MG cell lines expressing FLAG-tagged TRIM21 and the corresponding control treated with IFN-γ (100 units/ml) for 24 h. For the establishment of U87MG cell lines stably expressing FLAG-tagged TRIM21, U87MG cells were infected with a retrovirus encoding FLAG-tagged TRIM21 and the corresponding control vector (Mock). Anti-GAPDH antibody was used as an internal control.

Fig. 3. Knockout of TRIM22 promotes MHC-II expression. (A) Establishment of TRIM22-knockout U87MG cells with CRISPR/Cas9-based genome editing technology. Each expression level of TRIM22 protein was verified by immunoblot analysis. Each cell line was treated with IFN-γ (100 units/ml) for 24 h. Anti-GAPDH antibody was used as an internal control. (B) Immunoblot analysis of MHC-II protein in wild-type U87MG cells and TRIM22-knockout U87MG cells treated with IFN-γ (100 units/ml) for 24 h. Anti-GAPDH antibody was used as an internal control. (C) Flow cytometric analysis of cell surface MHC-II expression in wild-type U87MG cells (Gray), TRIM22 KO-102 cells (Blue), and TRIM22 KO-105 U87MG cells (Pink). Cells were untreated (upper panel) or treated (lower panel) with IFN-γ (100 units/ml) for 24 h. (D) Confocal immunofluorescence images showing the localization of endogenous MHC-II in wild-type U87MG cells and TRIM22-knockout U87MG cells. Cells were untreated (upper panel) or treated (lower panel) with IFN-γ (100 units/ml) for 24 h and stained with an anti-MHC-II antibody (green) and DAPI (blue). Scale bar, 20 μm, (E) Quantification of

fluorescence intensity at the cell surface of wild-type U87MG cells and TRIM22-knockout U87MG cells using ZEN2012 software (ZEISS). The *p* values for the indicated comparisons were determined using ANOVA followed by Dunnetts test (* $P < 0.05$).

Fig. 4. Knockout of TRIM22 does not affect mRNA level of MHC-II. qRT-PCR analysis of MHC-II mRNA levels in wild-type U87MG cells and TRIM22-knockout U87MG cells treated with IFN-γ (100 units/ml) for 24 h. Expression level was normalized to that of GAPDH. Shown are the means ± SDs from three independent experiments.

Fig. 5. TRIM22 suppresses the degradation of MHC-II protein. (A) Cycloheximide-chase assays of wild-type U87MG cells and TRIM22-knockout U87MG cells. Cells were cultured in the presence of cycloheximide (25 μl/ml) for the indicated times. Whole cell lysates were evaluated by immunoblot analysis. Anti-GAPDH antibody was used as an internal control. The results are representative of three independent experiments. (B) The intensity of the MHC-II bands was normalized to that of the corresponding GAPDH bands shown in (A) and is shown as a percentage of the normalized value at 0 h. The *p* values for the indicated comparisons were determined using ANOVA followed by Dunnetts test (* $P < 0.05$, ** $P < 0.01$). (C) A model for TRIM22 function in MHC-II expression. CIITA forms an enhanceosome at the MHC-II promoters and activates their transcription. Transcribed mRNAs are processed, exported to the cytosol, and translated to polypeptides by the ribosomes. The eIF4E binds to eIF4G and eIF4A to form the eIF4F complex. eIF4F complex binds to the 5’ cap of mRNA, allowing the recruitment of

ribosomes to initiate the translation, so-called cap-dependent translation. Since TRIM22 inhibits the binding of eIF4E to eIF4G and represses its cap-dependent translation, there is a possibility that MHC-II expression is negatively regulated through the TRIM22-eIF4E-eIF4G axis. Foreign antigens are phagocytosed and processed into small peptides that are subsequently loaded onto MHC-II, and this peptide-MHC-II complex is presented on the plasma membrane for recognition by T cells. Surface-expressed peptide-MHC-II complex can be internalized through the clathrin-independent endocytosis pathway and can be targeted for lysosomal degradation or can be recycled back to the plasma membrane. TRIM22 also enhances the stability of MHC-II proteins through an unknown mechanism, although its effect may be weaker than the inhibitory effect of a process that appears to be mediated by translation.

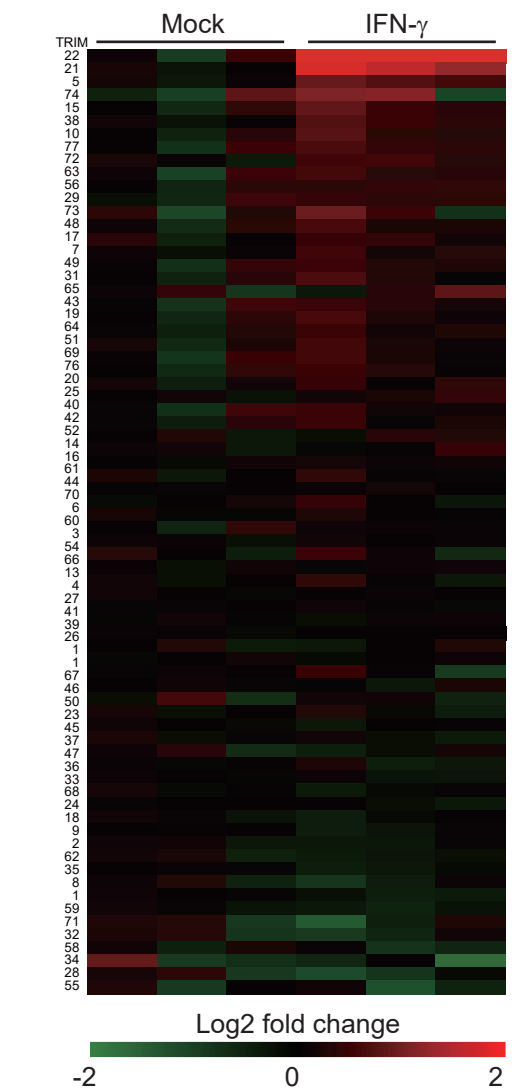

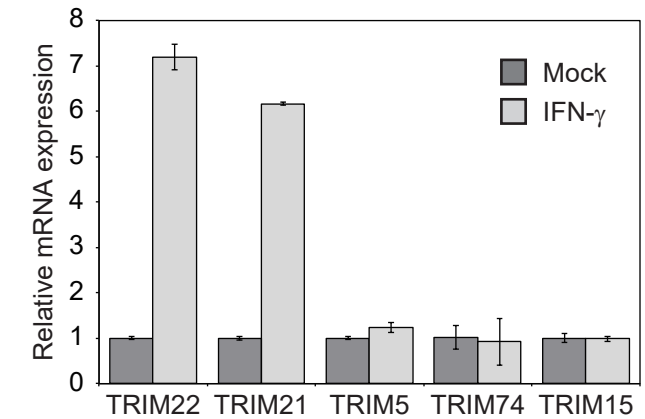

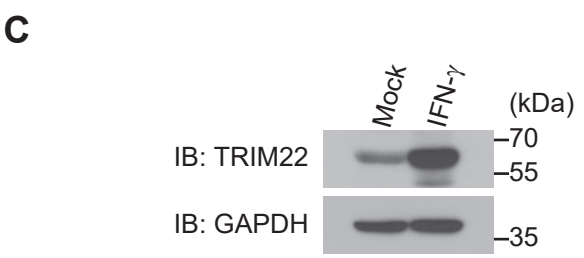

Inoue, A., et al. Figure 1

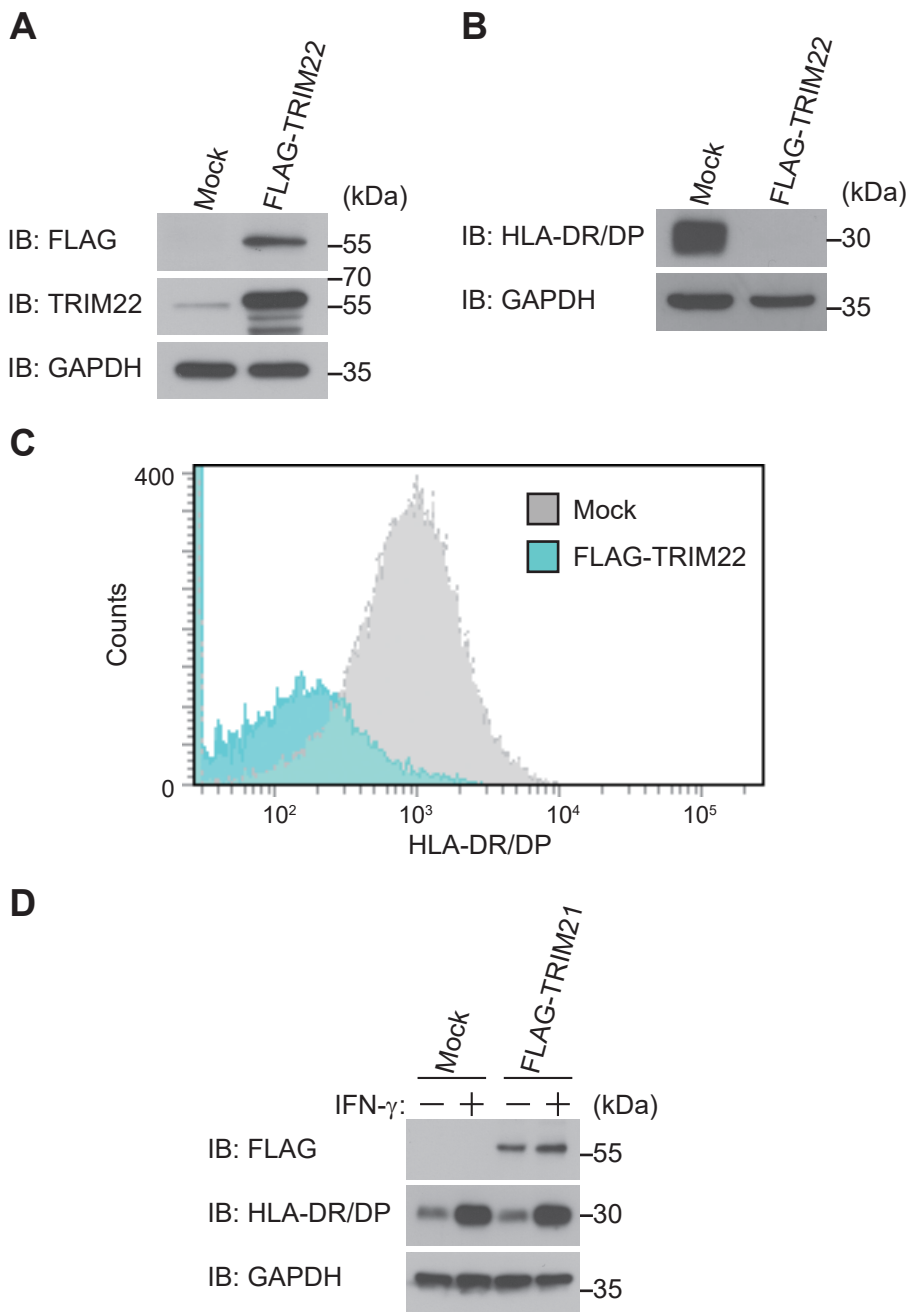

Inoue, A., et al. Figure 2

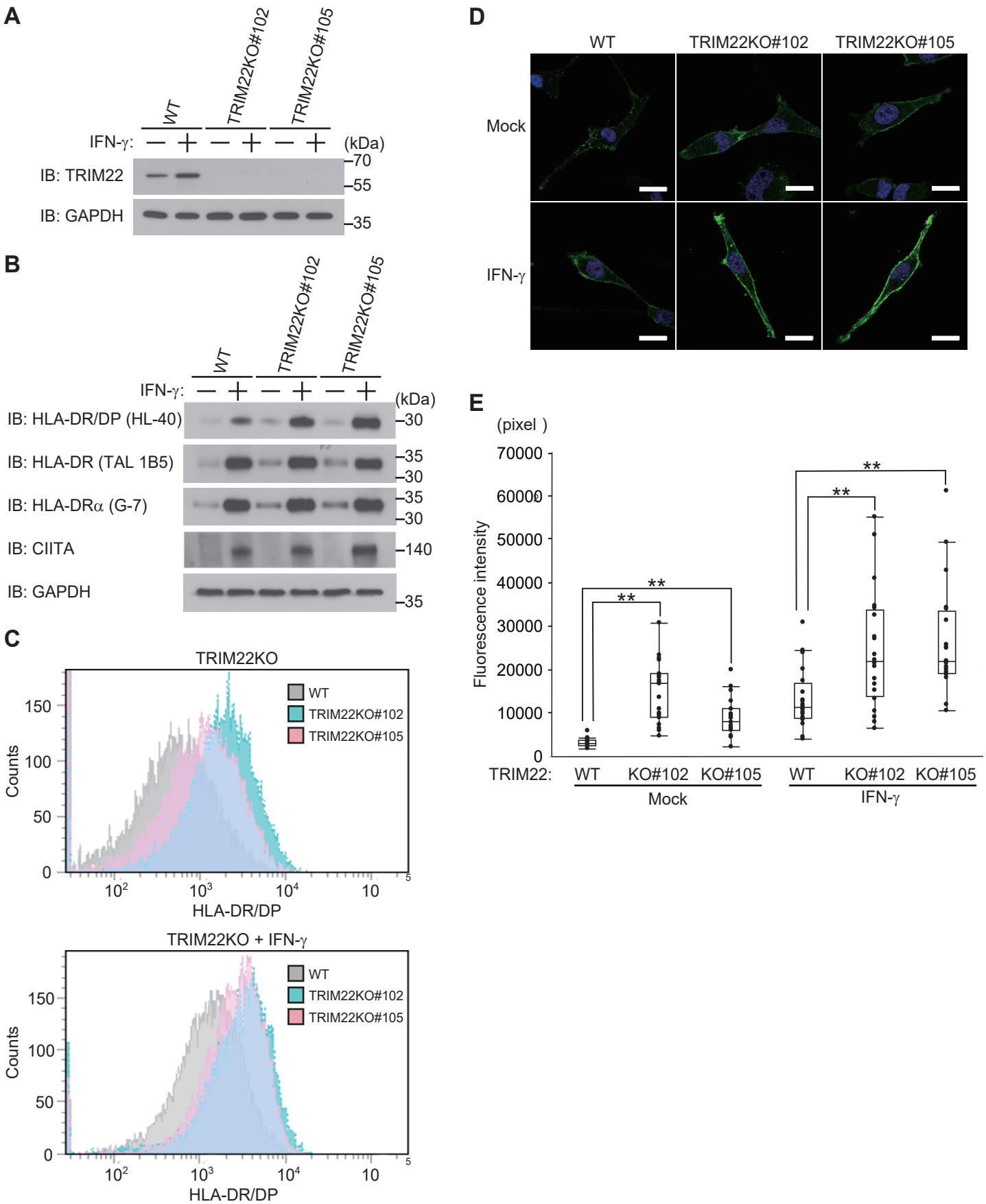

Inoue, A., et al. Figure 3

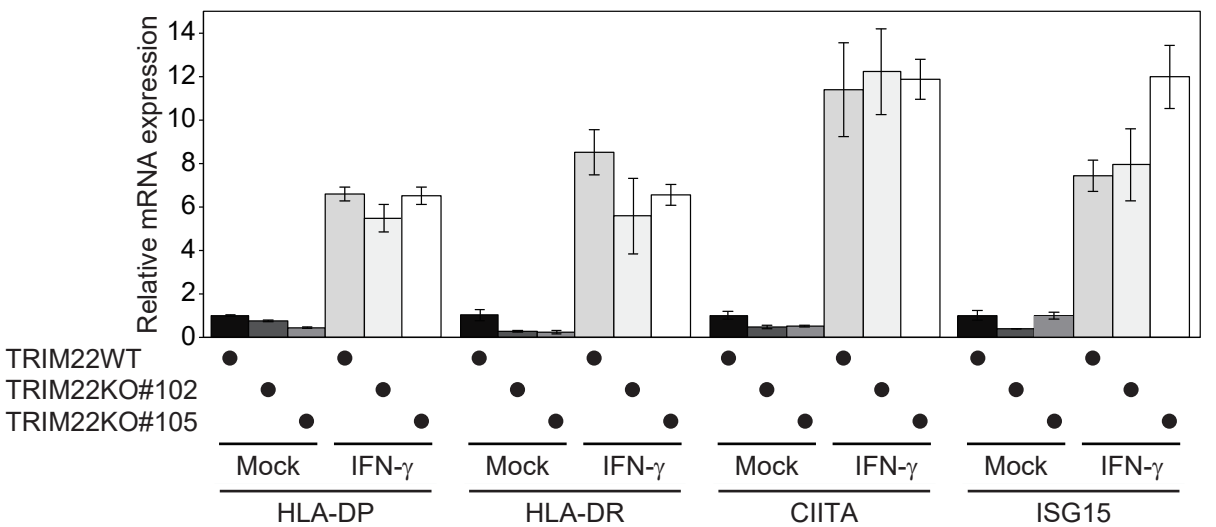

Inoue, A., et al. Figure 4

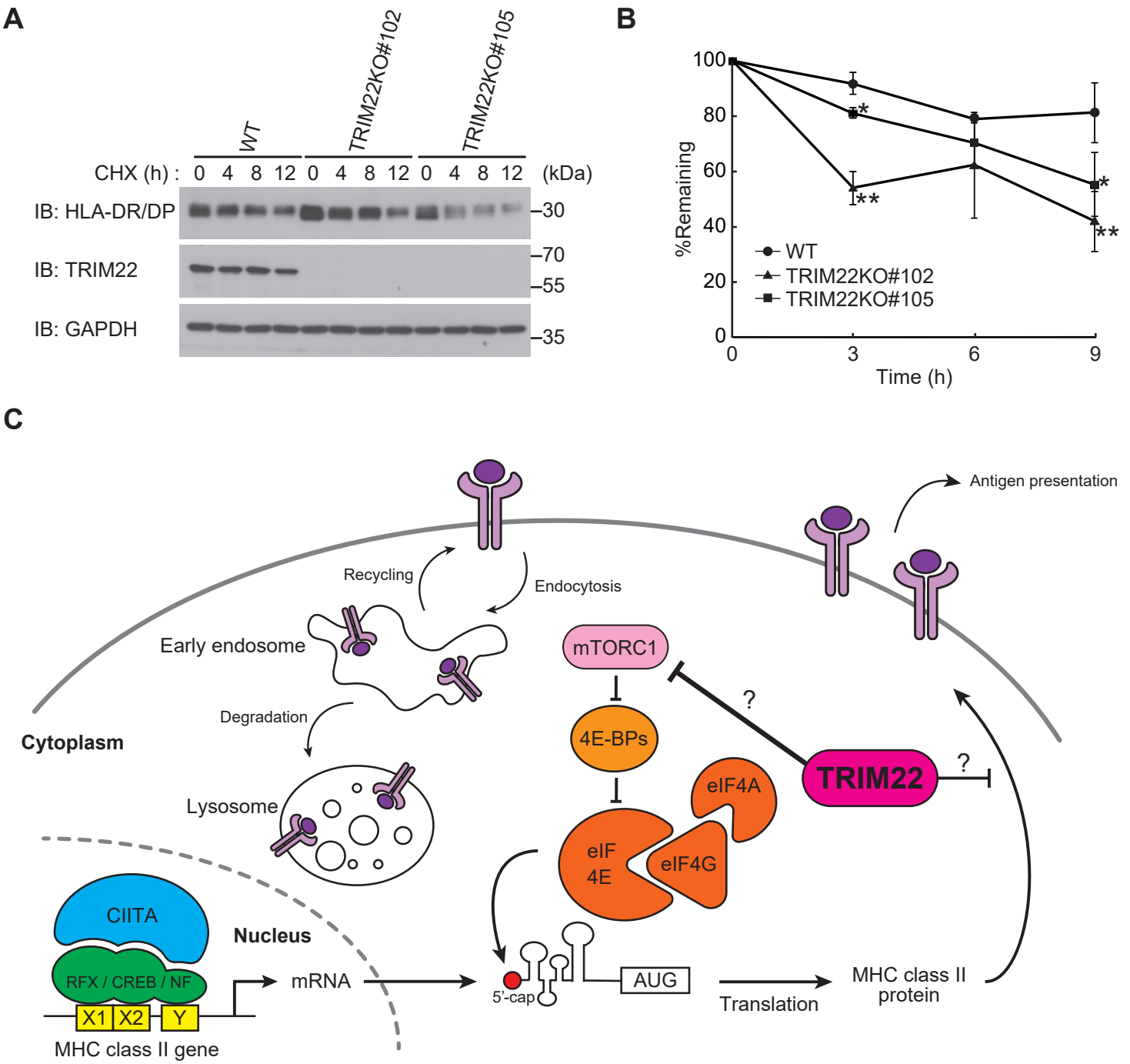

Inoue, A., et al. Figure 5

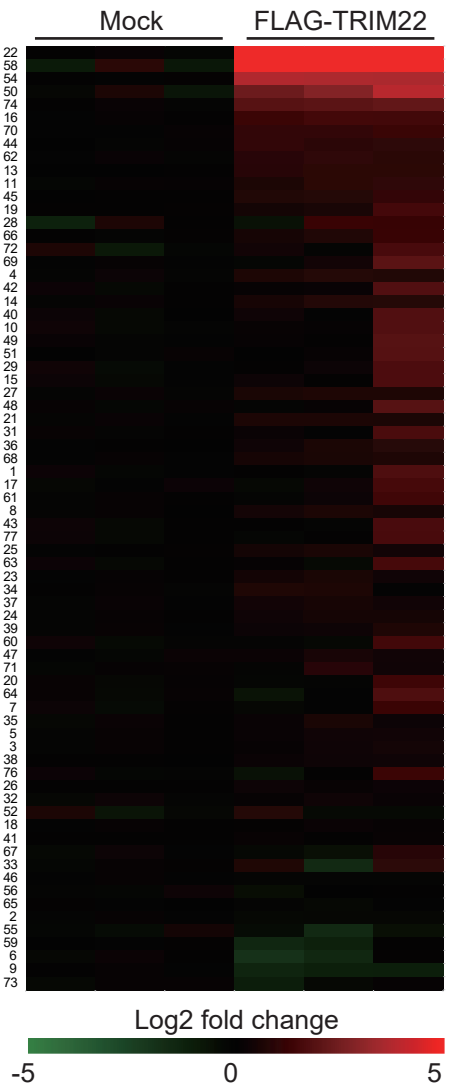

Supplementary Figure 1: Effect of TRIM22 overexpression on the expression of other TRIM family members. The mRNA expression of all TRIM genes was analyzed by qRT-PCR. The relative gene log2 expression changes are presented as a heat map. Expression levels in U87MG cells stably expressing FLAG-TRIM22 relative to the corresponding control were normalized for each TRIM gene. Green and red colors indicate lower levels and higher levels of gene expression, respectively.

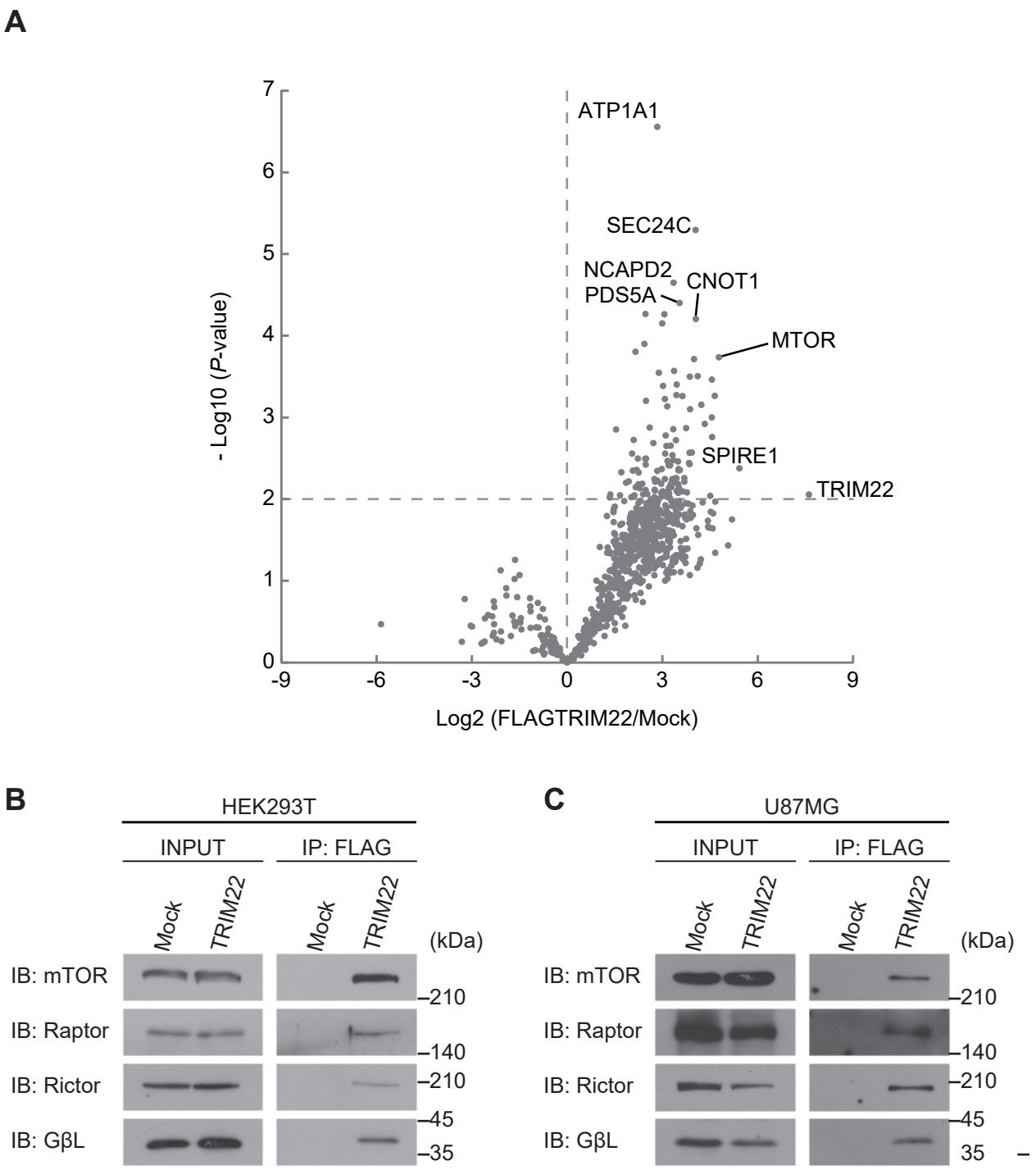

Supplementary Figure 2. Identification of TRIM22-interacting proteins. **(A)** Volcano plot showing the the results of LC-MS/MS analysis of HEK293T cells expressing FLAG-tagged TRIM22 (FLAG-TRIM22) or the corresponding control (Mock). n=3 (FLAG-TRIM22) or n=7 (Mock) biologically independent samples. Unpaired two-sided Student' s t-tests were used to calculate the *P* values for the volcano plots. **(B)** In vivo assay for interaction between TRIM22 and mTOR subunits in HEK293T cells. Lysates from HEK293T cells expressing FLAG-tagged TRIM22 (FLAG-TRIM22) or the corresponding control (Mock) were immunoprecipitated with anti-FLAG antibody and immunoblotted with the indicated antibodies. **(C)** In vivo assay for interaction between TRIM22 and mTOR subunits in U87MG cells. Lysates from U87MG cells expressing FLAG-tagged TRIM22 (FLAG-TRIM22) or the corresponding control (Mock) were immunoprecipitated with anti-FLAG antibody and immunoblotted with the indicated antibodies.

Supplementary Table 1. Primer sets used in this study

Gene symbol	Forward primer (5'-3')	Reverse primer (5'-3')
TRIM1	CCAGCCTCCGTGGTTCTTAAT	ACAGGTCAATTCAGACTCCAGT
TRIM2	TGCGCCAGATTGACAAGCA	GCACCTCTCGCAGAAAGTG
TRIM3	GCGACCTGGAGACCATTTGT	GCTACTGCCGATGTGTTCCTG
TRIM4	TGAGAATCAGCACGGAGTTTTC	CCTGGTCAACACTTCTTTTGGA
TRIM5	AAGTCCATGCTAGACAAAGGAGA	GTTGGCTACATGCCGATTAGG
TRIM6	ACTGGGTTGACGTGACCCT	TCCCACAAACCTCACTTGTCT
TRIM7	TCCATGTTCAAGTCCCTCTCC	GGCCAGGTTCTCATTCTGCT
TRIM8	CGTGGAGATCCGAAGGAATGA	CAGGCGCTTGTCTGACTCG
TRIM9	GTGTGCGGCTCCTTCTATCG	GCTGTATAGGCTCATCTTGTCCA
TRIM10	CTGCCCCATCTGTCAGGGTA	GGTATCTCACAGTAGCGGGTAA
TRIM11	TGGCTGCTCTGGAAGAATTAG	TCTACTCTCTGTTCCTGTCCTC
TRIM13	GTTTTGCCTTGCTCCCACAAC	TCCTTACGGCATGTAGGACAC
TRIM14	TGAAGGGGAAATTCACTGAACTC	AGCCTCTGGACAGGATCGG
TRIM15	TCCCTGAAGGTGGTCCATGAG	CAGGATCTTGCCCGAGGATT
TRIM16	GTCCTGTCTAACCTGCATGGT	GGCAGTATCGCCAGTTGTG
TRIM17	CGGACAGATTGAAGTGCTAAGA	CTCTCATACAGGAGGAGGTAGG
TRIM18	CTGACCTGCCCTATTTGTCTG	GCACAGTGTGATACTAGGATGC
TRIM19	TGGGAGCTTACTGGGTTAGA	GGATCAAGGAGGGAGGTTAATG
TRIM20	TAAGACCCCTAGTGACCATCTG	TTCCCCATAGTAGGTGACCAG
TRIM21	TGGCTGAGAAGTTGGAAGTG	CAAACTCTGCGTGAATCCTAGA
TRIM22	GTCACCAAACATTCCGCATAAA	TGATGTCATCTTCCAGCTTCTC
TRIM23	TGGTTGTAAACAAGCTCGGAG	ACTCTAGCACCTTCACTACAGC
TRIM24	GAAGTGGCTGGACTCTCTAAAC	TGCCGTAACCGGTATGTAATC
TRIM25	AATCGGCTGCGGGAATTTTTC	TCTCACATCATCCAGTGCTCT
TRIM26	TGCACTACTACTGTGAGGACG	TCCTTAGGGTACTCAGGTGGT
TRIM27	CAGAACCAGCTCGACCATTTA	CCCAAACAATCTTCTCCCTCTC
TRIM28	TTTCATGCGTGATAGTGGCAG	GCCTCTACACAGGTCTCACAC
TRIM29	CTGTTCGCGGGCAATGAGT	TGCCTTCCATAGAGTCCATGC
TRIM31	AACCTGTCACCATCGACTGTG	TGATTGCGTTCTTCCTTACGG
TRIM32	GCGGTCAGCAGGAATTTG	CAGATGGTATGGCCACAGT
TRIM33	ATGTGGAGAGTGGCTATGTAAGA	GGGCGTTGACCAGATGCTC
TRIM34	GACGCTGGATAAGTTTGCAGA	CCACCCATACGCACCATTTC
TRIM35	TGAAGGAGGACGACGTTTCTT	GCCCAGGTACTTGCAGACATC
TRIM36	GAGCTGTTTACCCACCCATTG	CTGATCCCACATCGTTGAATGA
TRIM37	GAGGGAGAACTCATGGAAGATG	GGTAGCAGCGGAGCATAAA
TRIM38	GAGCCTGATGACGAACCCAG	TCTTGATCCGTCTCTTTGAGGG
TRIM39	GAAAGGGCGAGTTGACTCCAC	GGCTGCATATTTGTCCCCATT
TRIM40	ACATCTCTTCTGTCGAGTGTGC	GGCAGATATAGCCTGTCCCTA
TRIM41	CTGCCGAGTTTGTGTAACCCA	CTCCTCCATGTCACCCTCGTA
TRIM42	GGCCAATGATCCCAACTGTAA	AGCAGCGGCTCTCATAGTAGT
TRIM43	AGGGAACCATCACCGAAAATG	TTGTTTGCCTATGGGTCCCAC
TRIM44	CCATCTGGCCGAATACGTCC	TGCCTCGCTTTCTATCTCCCT
TRIM45	AACTCAGGCAAGACTCACTGC	CCCTCGGATGTCCACTACTG
TRIM46	TTCCGACCCAAGGGCCTTAT	AGAGTTGACATACCAGGCGTT
TRIM47	CTGAGCAGTCCAAAGTCCTGA	CTACGGCTGCACTCTTGATG
TRIM48	GGATGTGACCGTCAAAATCCG	CACCCAAGACTAAAGAGTCCCT
TRIM49	ATCTTACAGGTCTTTCAGGGGG	GCACTGGACAAGAAATGGGAT
TRIM50	GGCCCTTAGAAGGCGCATT	GCAGGGTCCAACTTGAGAGG
TIRM51	GGCCCTGTTTGTACCTCAACT	TTCTCTGCCGCGTTGTCTTC
TRIM52	ATGGCTGGTTATGCCACTACT	CTCGTCCTCCTTACTCCACAG
TRIM54	ATCGTGCAGGCATGAGGTTG	CCTCGCACATGAGGTGCTG
TRIM55	TTGTCAGCACAACCTGTGTAG	CCCATGTCTATCCAAAACCACTT
TRIM56	GCCTGCATACCTACTGCCAAG	GCAGCCCATTGACGAAGAAGT
TRIM58	TACCAGGTAAAGCTCCAGATGG	GAAAGCCACGATGCTTCTCAA
TRIM59	GACACACACTGGACAGATCTTA	ACTGGAGAACAGCTTCCTTATC
TRIM60	CTCCAAGAGGAGTCTAGCTGT	TCCTTCCAGGATACACTGAGG

Gene symbol	Forward primer (5'-3')	Reverse primer (5'-3')
TRIM61	TCTGTCAGAAAGACCTAGAGCTT	CACGGTGCATTGTATTCCTCC
TRIM62	CGAGCAGCATCAGGTCACC	CCAGTTGTCGCTTGAGCAG
TRIM63	CTTCCAGGCTGCAAATCCCTA	ACACTCCGTGACGATCCATGA
TRIM64	TTCCTCCTTCCTCCTTCTCTT	GCTCTCGCACATAGTGTCTTAG
TRIM65	CGCCAACCGTCACTTCTATCT	ACAGGGTCAGGGTCCTACC
TRIM66	TCCCGGAGACTTCACCTTGTA	GTTCCACCACTAGGCAGCTAT
TRIM67	CGTGTCCCGAGCATGAAATG	CCTGAGATAGTTGTGCCTTGTG
TRIM68	GGAGCCCATGAGCATTGACT	GACAGGTGTAACCCCAGTTCT
TRIM69	CTTGCCATCCAACAGGGTCAA	TTCCTTGTGAGCAGCAATAGC
TRIM70	GCACCAAATCTCCCTCATCTT	CTCTTGAAGGTTCCTGGTCATC
TRIM71	GTACCCATCTGTCGTGAGTGC	CGGCTTTGACCTCCGACTG
TRIM72	GAGGTGGATGTTGGCGACAA	CCGAAGCTCAGGTAAAGGC
TRIM73	CAGGAGCAGAAGAAGGTGGATG	CCGCACTGTAGCATTAGGGACT
TRIM74	CAGGAGCAGAAGAAGGTGGATG	AACTCATGGTGGTCCTCATTTCC
TRIM76	CAGGTACTAACCACGGAGAAAG	CCCAGTAATCGGAGGTGTATTT
TRIM77	AGCCTGGACAAAGAGGAATG	GGGAGGTAGAGAAGAGACTGAA
HLA-A	CGACGCCGCGAGCCAGA	GCGATGTAATCCTTGCCGTCGTAG
HLA-B	GACGGCAAGGATTACATCGCCCTGAA	CACGGGCCGCCTCCCACT
HLA-C	GGAGACACAGAAGTACAAGCG	CGTCGTAGGCGTACTGGTCATA
HLA-DP	GATTTCTACCCAGGCAGCATT	GGTCATTTCCAGCATCACCAGGA
HLA-DR	CCGATCACCAATGTACCTCCAG	CAGGAAGGGGAGATAGTGGAAC
CIITA	CTGGCTGGAGAAGAAGAGATTG	AGTTCCGCGATATTGGCATAA
NLRC5	GGACCCTAGAGCACCTATCA	TTGGCGTTCAGCCATTCT
RFX5	CCCACAAGAAGCCAGAGAGA	GGCCGAGCTCTCAACTACAC
RFXB	GAAGCCGACTCTGGCTACAC	GGTTGCTCTGGAAGAGCTTG
RFXAP	GATCTTTTGGGGATCGTCCT	TGCTGTTTCTGTAAAAATTGCAC
NF-YA	GAGTCTCGGCACCGTCATG	TTCATCGGCTTGGTTTGGA
NF-YB	AGGTGCCATCAAGAGAAACG	TGTTGTTGACCGTCTGTGGT
NF-YC	AGGTGCGCCAGTCTGTAACT	CCTTCTCCAACCTGCATTGT
CREB	TGCAGCTGTAACAGAAGCTGA	AGAGTTACGGTGGGAGCAGA
ISG15	GAGAGGCAGCGAACTCATCTT	CCAGCATCTTCACCGTCAGG
CIITApI	TGACCCTACTAGAGAAAGGAGAC	CAACTCCATGGTGGCACA
CIITApIII	CTGCCTGGCTGGGATTC	CAACTCCATGGTGGCACA
CIITApIV	AGCTGCCACAGACTTGC	CAACTCCATGGTGGCACA
GAPDH	TGCACCACCAACTGCTTAGC	GGCATGGACTGTGGTCATGAG
HPRT1	TGACACTGGCAAAACAATGCA	GGTCCTTTTCACCAGCAAGCT
dSeq	AACCTCTGAGCCTAGATTGTG	CCTGCAGCTTTTCCTGTAAG